Available online at www.sciencedirect.com
SCIENCE DIRECT®
Journal of Photochemistry and Photobiology A: Chemistry 180 (2006) 46–53
Journal of Photochemistry and Photobiology A:Chemistry
www.elsevier.com/locate/jphotochem

Photochemical transformation in poly(acrylic acid)/poly(ethylene oxide) complexes

Halina Kaczmarek*, Aleksandra Szalla

Faculty of Chemistry, Nicolaus Copernicus University, Gagarin 7, 87-100 Toruń, Poland

Received 18 March 2005; received in revised form 3 September 2005; accepted 19 September 2005
Available online 26 October 2005

Abstract

The poly(acrylic acid)/poly(ethylene oxide) (PAA/PEO) complexes with different stoichiometric ratio were obtained from aqueous solutions. The chemical structure of these blends in solid state and the interactions between components has been studied using mainly FT-IR spectroscopy. The miscibility of components was proved also by differential scanning calorimetry (DSC). The films of both pure polymers and their blends at different compositions were UV-irradiated ($\lambda = 254$ nm) in air atmosphere. The course of photochemical transformations has been monitored by absorption spectroscopy (FT-IR, UV–vis), DSC, X-ray diffraction and thermogravimetry, which was also applied for estimation of the thermal properties of samples studied.

It was found that photooxidative degradation is less efficient in PAA/PEO complexes than that in PAA and PEO exposed separately. The most photostable was PAA/PEO (50/50) blend. PAA disturbs crystallization PEO in the blends but changes in crystallinity degree of PEO/PAA during UV-radiation were negligible.

Thermal stability of PAA/PEO complexes is lower comparing to pure components but UV-irradiation does not cause significant changes in thermal resistance of blends studied.

Keywords: Poly(acrylic acid); PAA; poly(ethylene oxide); PEO; Polymer blends; photooxidative degradation

1. Introduction

Poly(ethylene oxide) (PEO) is one of the most extensively studied crystalline, water soluble polymers. In general, it has been used as a component of innumerable polymer blends for the purpose of analysing properties, such as miscibility, crystallization processes and interaction parameters.

Poly(acrylic acid) (PAA) which is characterised by a biocompatibility with biomaterials, has also a wide applications, e.g. as an agent in lattices and adhesives and in the formulation of pharmaceutical products, cosmetics and agricultural chemicals.

It is well known that mixing of the solutions of two complementary polymers: polybase with polyacid can lead to formation of intermacromolecular complexes [1–4]. The structure of these complexes is stabilised by electrostatic interactions (polyanion–polycation), hydrogen bonds between carboxyl protons and carbonyl oxygen atoms or by hydrophobic interactions between the polymer chains. The mixing of water solutions of poly(acrylic acid) and poly(ethylene oxide) in the neutral or acidic conditions [5] should lead to the formation of complexes based on hydrogen bonding between carboxylic group from PAA and the ether oxygen of PEO (–OH. . .O<), while in alkaline environment [6,7], where the carboxylate ions exist in PAA, we can expect the electrostatic interactions between them and mixed dipole–ion interactions. The strong interactions lead to miscibility of components, which is not very typical in many polymer blends. Such compositions are characterised by different properties than immiscible and incompatible blends as well as than properties of pure polymers.

The influence of hydrogen bonding on miscibility of polymeric blends and their properties was a subject of many publications [8–13]. The strength of hydrogen bonds depends on many factors: the acidity of the proton donor, the basicity of the proton acceptor, accessibility of acceptor and donor (steric hindrances), polymer crystallinity, chain stereoregularity and flexibility as well as preparation conditions (temperature, annealing, etc.).

The different methods are used for studying of interpolymer interactions responsible for miscibility: often used are IR and

* Corresponding author. Tel.: +4856 6114312.
E-mail address: halina@chem.uni.torun.pl (H. Kaczmarek).

1010-6030/$ – see front matter © 2005 Elsevier B.V. All rights reserved.
doi:10.1016/j.jphotochem.2005.09.014

NMR spectroscopy [14,15]. The miscibility of components in polymer blend can be also estimated using viscometry [16,17], differential scanning calorimetry (DSC) [18,19] and dynamic mechanical analysis (DMA, DMTA) [20,21]. Also microscopic methods (including optical microscopy, SEM and AFM) are applied [22,23]. Moreover, it was recently published that determination of interfacial tension is useful for characterisation of system miscibility [24].

The knowledge about hydrogen bonds in synthetic polymers can be applied in explanation of behaviour of biopolymers (such as proteins, polysaccharides and nucleic acids), which are components of living organisms.

In our previous works, we found the effect of hydrogen bonds on photochemical stability of poly(acrylic acid)/poly(vinyl pyrolidone) [7] and poly(ethylene oxide)/poly(vinyl chloride) blends [23].

The aim of this work was to study the photochemical reactions in the complexes of poly(acrylic acid) with poly(ethylene oxide) formed in solid state. The experimental techniques employed in this study are Fourier transform-infrared (FT-IR) and UV–vis spectroscopy, differential scanning calorimetry (DSC), X-ray diffraction and thermogravimetric analysis (TGA).

2. Experimental details

2.1. Polymers

Poly(acrylic acid) (PAA) with $M_w = 100{,}000$ and poly(ethylene oxide) (PEO) with $M_w = 100{,}000$ were purchased from Aldrich Chemical Co.

The concentration of PAA solution prepared was checked by titration of 0.1 mol/l NaOH with phenolphthalein. PEO was purified by dissolution in distilled water and centrifugation from slightly turbid, insoluble contamination. Clear solution was cast to Petrie's plate and solvent was evaporated to sample dryness. Before use, the polymer was dried in vacuum at room temperature.

2.2. PAA/PEO complex preparation

The pure PAA and PEO were dissolved in water at room temperature. PAA/PEO complexes were prepared by mixing of different amounts of the components to obtain blends with required molar ratio of polymers. pH of PAA/PEO solutions was varried from 3.72 (for 1% PAA) to 4.80 for PAA/PEO (10/90) blend. Solutions were directly poured out onto CaF_2 spectrophotometric windows (for IR) or onto quartz plates (for UV–vis). After solvent evaporation, the samples were dried in a vacuum to a constant weight. The film thickness was about 10 μm.

2.3. UV-irradiation

Obtained thin films were exposed to a low-pressure mercury vapour lamp (TUV 30 W, Philips, Holland). Samples of the same thickness and surface area were placed at 6 cm distance from the light source. The light intensity, measured with an IL 1400A Radiometer (International Light, USA), was 2.98 mW/cm^2. Times of irradiation were 0.5, 1, 2, 4, 6 and 8 h. All irradiation were performed at room temperature in air atmosphere.

2.4. Methods of studies

The structure of complexes in solid state has been studied using FT-IR spectroscopy. Photochemical changes in polymer films were recorded by both infrared and electronic absorption spectroscopy using FT-IR Genesis II Spectrophotometer (Mattson, USA) and UV PC 1600 spectrometer (Shimadzu, Japan), respectively.

DSC thermograms were obtained on a Polymer Laboratories PL-DSC differential scanning calorimeter. Samples were first heated from 20 to 200 °C at a heating rate of 10 °C/min (run I). Then, the samples were cooled to −50 °C at the same rate (run II) and heated again to 200 °C (run III). The apparatus was calibrated with indium standard under nitrogen atmosphere. The melting temperature (T_m) and melting enthalpy (ΔH_m) were determined from the DSC endothermic peaks for third run.

The degree of crystallinity (X_c) was calculated from the ratio of the enthalpy of melting of the sample studied (ΔH_m) and the enthalpy of melting of 100% crystalline, pure PEO ($\Delta H_m^\circ = 203.45$ J/g [25]):

$$X_c = \frac{\Delta H_m}{\Delta H_m^\circ} \tag{1}$$

On the base of the experimental values of T_g for pure polymers, T_g for blends were calculated from Fox Eq. (2):

$$\frac{1}{T_g} = \frac{w_1}{T_{g_1}} + \frac{w_2}{T_{g_2}} \tag{2}$$

where T_g is the glass temperature for blend, T_{g1} – the glass temperature for polymer 1, T_{g2} – the glass temperature for polymer 2, w_1 the weight fraction of polymer 1, and w_2 is the weight fraction of polymer 2.

These calculated T_g values were compared to experimental T_g for blends and the components miscibility was estimated.

X-ray analysis was carried out on a Phillips X'Pert PRO diffractometer using Cu Kα, Cu-filtered radiation in the diffraction angle range: $2\theta = 4$–80°.

Thermogravimetric measurements were done on a Thermal Analysis SDT 2960 Simultaneous DSC-TGA analyser in dry nitrogen atmosphere. All blends were heated from 20 to 600 °C at 6 °C/min rate.

3. Results and discussion

3.1. Studies of PAA/PEO structure by FT-IR spectroscopy

The interactions of the ether oxygen atoms from PEO with the carboxylic acid groups of PAA were analysed by FT-IR spectroscopy. The spectra in whole measured region (4000–800 cm^{-1}) for pure solid components (PAA, PEO) as well as for PAA/PEO blends at 80/20, 50/50 and 20/80 molar ratios are shown in Fig. 1.

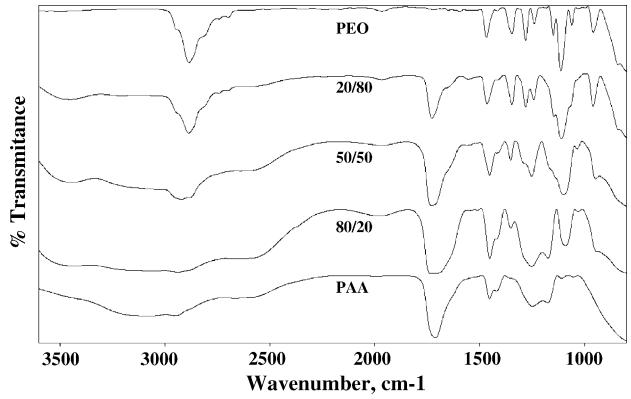

Fig. 1. FT-IR spectra of unirradiated PAA, PEO and PAA/PEO (20/80; 50/50; 80/20) blends obtained from 0.1% aqueous solution (films on CaF_2 crystal).

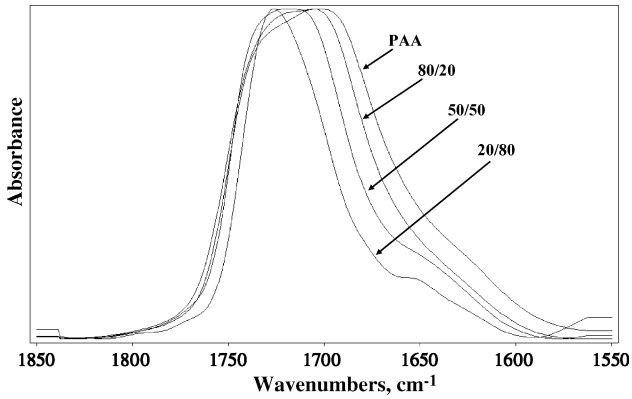

Fig. 3. Carbonyl band of unirradiated PAA and PAA/PEO complexes at different molar ratio, normalised.

The hydroxyl region of spectra for these samples is presented in Fig. 2. In PAA spectra, we observed a broad, intensive band corresponding to the overlapped components at ca. 3555 and 3171 cm^{-1}. These bands are related to the free hydroxyl groups and the hydroxyls forming hydrogen bonds, respectively [8,13].

In PAA/PEO blend, the intensity of band at 3171 cm^{-1} decreases and the band at 3555 cm^{-1} shifts to a lower wavenumbers with the increase of PEO percentage amount in the sample.

The decrease of the band at ca. 3171 cm^{-1}, is caused by changes in hydrogen bonding, resulting of PAA/PEO interactions (instead of self-associated hydrogen bonds in PAA) and also by the decrease of the acidic group concentration (due to smaller PAA content). The shift of the band corresponding to free hydroxyl groups (from 3555 to 3485 cm^{-1}) indicates that, new type of interactions in PAA/PEO appears.

It suggests, that besides of free and bonded OH groups existing in PAA (structure I), also interpolymer hydrogen bonds between PAA and PEO are formed in the blends (structure II):

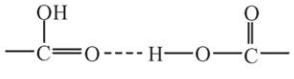

Structure I – Intrapolymer hydrogen bond among PAA molecules (dimeric form).

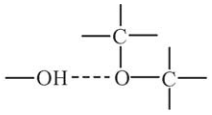

Structure II – Interpolymer hydrogen bond between PAA and PEO (complex form).

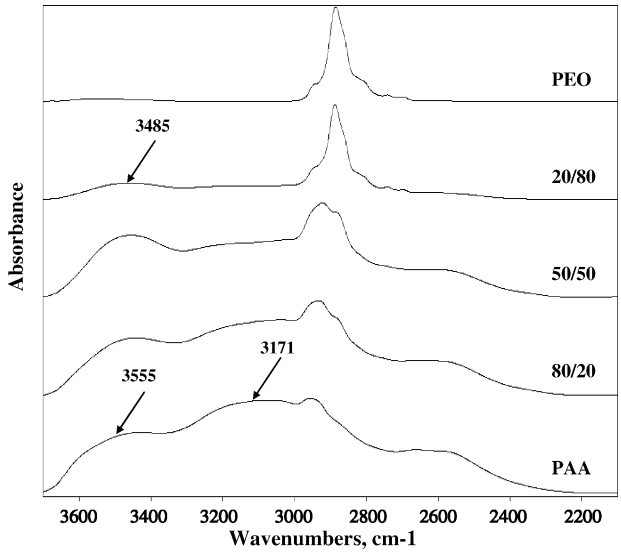

Fig. 2. FT-IR spectra for pure, unirradiated components and PAA/PEO blends in the region of 3700–2200 cm^{-1} (films on CaF_2 crystal).

The shift of free and bonded hydroxyl bands indicates that the chemical surrounding of OH groups in the blend is different than that in PAA alone. It is seen from comparison of structures I and II, that in case of hydrogen bonds, the ether oxygen atom availability from PEO is lower than carbonyl oxygen in PAA. However, the shape of hydroxyl band indicates that both free and associated hydrogen bonds exist in PAA/PEO blend.

The spectrum of PAA and its blends at different molar ratio in carbonyl region (1850–1550 cm^{-1}) also show shift of band maximum (Fig. 3) resulting of changes in polymer interactions.

The broadening of the carbonyl stretching vibration band is attributed to the formation of the intra- and intermolecular hydrogen bonding besides of free carbonyl groups existing together. With the increase of PEO amount in the blend, the intensity of this band decreases. The maximum of carbonyl band in PAA lies at 1717 cm^{-1}, but in the blends, it shifts to higher wavenumbers (from 1717 to 1728 cm^{-1}). Thus, one can conclude, that some self-associated hydrogen bonds (PAA–PAA) are replaced by new inter-associated bindings: PAA–PEO, as it was suggested on the observed above changes in hydroxyl region.

In case of PEO-rich blends (e.g. in samples containing more than 70% PEO), the carbonyl band narrows, which indicates that

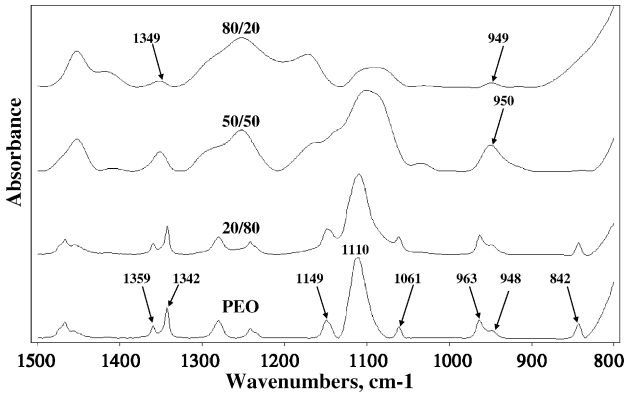

Fig. 4. FT-IR spectra for pure PEO and PAA/PEO blends in the region of 1500–800 cm^{-1}.

the dominant PEO impedes the interaction between carboxylic groups, i.e. PAA–PAA interactions. Small PAA amount in such blends is also the reason of less polyacid-polyether interactions.

The 1400–800 cm^{-1} range is useful for estimation of ether bond amount and macrochain order (crystallinity degree). Spectra of PEO and its blends in this region are shown in Fig. 4.

The bands at 1149, 1110 and 1061 cm^{-1} can be assigned to ether groups. Other bands in this region are characteristic for crystalline state of PEO [19]. The bands at 1359 and 1342 cm^{-1} are associated with CH_2 wagging motion; the 963 and 948 cm^{-1} bands are due to CH_2 rocking vibrations. These bands are sensitive to chain conformation changes [5].

All these bands are present also in blends with PEO dominant content (80 and 90%) but some changes in complexes containing lower PEO amount (<60%) were observed. The 1359 and 1342 cm^{-1} doublet in PEO spectrum is replaced by the single 1349 cm^{-1} band in PAA/PEO blends. Similarly, the 963 and 948 cm^{-1} bands are replaced by one band at 950 cm^{-1} in complexes. It means that the PEO crystallization is hampered in the presence of PAA. Another band at 842 cm^{-1}, associated to mixed motion of CH_2 rocking, C–O–C deformation and to the gauche form in the 7/2 helical structure of PEO, disappears in the blend containing above 60% PAA. Thus, PAA causes the disturbances in PEO helical structure.

3.2. Effect of UV-irradiation on PAA/PEO complexes FT-IR spectroscopic studies

The hydroxyl region in FT-IR spectra is not very useful for quantitative evaluation of UV-irradiation effect because of overlapping of bands due to free, self- and inter-associated OH groups as well as new functional groups formed resulting of photooxidation. Thus, we focused on interpretation of band attributed to carbonyl groups, although, this band is also complicated.

The maximum of carbonyl band in all UV-irradiated samples shifts to a lower wavelength (Table 1). It indicates the formation of new products of photochemical reactions in PAA complexes. Moreover, the band due ether group in PEO at about 1100 cm^{-1} also shifts after 8 h UV-irradiation but these changes are irregular.

Table 1
Main carbonyl and ether peak position in FT-IR spectra for PAA, PEO and their blends before and after 8 h UV-irradiation

Sample composition PAA/PEO	[C=O] (cm^{-1})		[COC] (cm^{-1})	
	0 h	8 h	0 h	8 h
100/0	1717	1707	–	–
80/20	1711	1702	1090	1088
50/50	1723	1714	1101	1097
20/80	1728	1726	1109	1110
0/100	–	–	1110	1113

The total amount of carbonyl and ether groups in UV-irradiated samples was calculated as integral intensity of absorption band (i.e. as surface area of peak) at 1550–1850 and 1052–1160 cm^{-1} ranges, respectively (Figs. 5 and 6).

The amount of carbonyl group decreases in pure PAA and its blends during UV-irradiation (negative values, Fig. 5). The reason is destruction or abstraction of side carboxylic groups from PAA chains. These changes depend on exposure time and sample composition. The highest drop in carbonyl groups amount was found for PAA, whereas in PAA/PEO blends these changes are smaller. It should be pointed out that the smallest decrease of total carbonyl group content was observed in PAA/PEO (50/50) complex, which leads to conclusion that this composition is more photostable than others are.

The detail analysis of FT-IR spectra in range of ether bond vibration (C–O–C) from PEO confirms above conclusion (Fig. 6). The slight decrease of intensity of band with maximum at 1110 cm^{-1} is caused by the destruction of PEO (mainly breaking of C–O bonds in main chain), connected with evaporation of volatile, low-molecular degradation products. The changes are highest in pure UV-irradiated PEO, while the smallest decrease of C–O–C amount was found for PAA/PEO (50/50) blend.

Absorption bands attributed to crystalline phase (at 1359, 1342, 963 and 948 cm^{-1}) in blends with PEO majority slightly

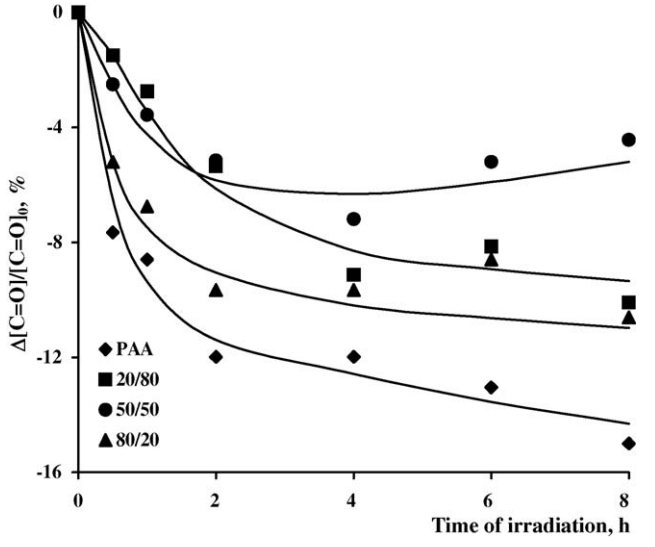

Fig. 5. The relative changes of carbonyl group amount in PAA and PAA/PEO blend during UV-irradiation (measured as integral intensity of carbonyl band at 1550–1850 cm^{-1} ranges).

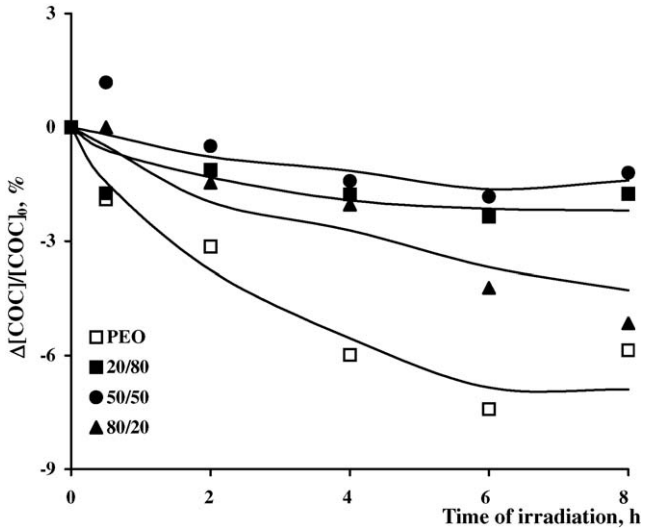

Fig. 6. The relative changes of ether group amount in PEO and PAA/PEO blend during UV-irradiation (measured as integral intensity of ether band at 1052–1160 cm^{-1} ranges).

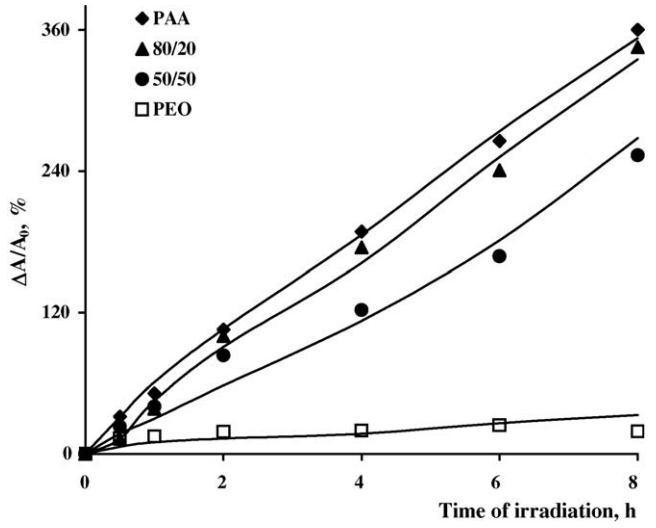

Fig. 7. The relative changes of chromophores amount in PAA, PEO and its complexes vs. irradiation time (measured as relative changes of absorbance at 290 nm).

decreases during UV-irradiation. It suggests the decrease of crystallinity during UV-irradiation. For PAA-rich samples such estimation of crystallinity changes is not possible because the bands characteristic for PEO crystallities appear at different position, which was described in Section 3.1.

3.3. Effect of UV-irradiation on PAA/PEO complexes UV–vis spectroscopic studies

UV–vis absorption spectra supply an information about chromophores formation in UV-irradiated samples. Spectrum of pure PEO does not contain absorption maximum at 200–800 nm ranges (only tail of main band with maximum below 200 nm is seen). In PEO and PEO-rich blend spectra, the relatively high background appears, which is caused by sample crystallinity.

PAA exhibits absorption at 209 and 290 nm due to $n \rightarrow \sigma^*$ and $n \rightarrow \pi^*$ transitions in carboxylic group existing in each polymeric unit. These bands are somewhat shifted but exist in PAA/PEO blends. The first band at 209 nm is very intensive and it requires very thin films for quantitative calculations, thus, we focused on 290 nm band.

UV-irradiation leads to systematic increase of absorbance at whole range of measurement (200–800 nm), although no new distinct maximum was observed. Changes of absorbance calculated at 290 nm, after turbidity elimination, allow to compare the course of photochemical reactions leading to changes in chromophores concentration caused in all samples by competitive reactions: COOH abstraction or new chromophores formation (such as carbonyl groups or double bonds) (Fig. 7).

The changes of absorbance at 290 nm during UV-irradiation are largest in pure PAA and blends with dominant PAA amount. Even in PAA/PEO (50/50) sample, the rate and efficiency of photoreaction monitored by changes of absorption 290 nm was high. On the contrary, very low absorbance changes were found for UV-irradiated PEO and compositions containing 70–90% PEO. It can be explained by the different main photochemical reaction occurring in PEO and PAA (thus also in PEO-rich blends and PAA-rich blends). PEO undergoes mainly random chain scission upon UV-radiation, whereas more competitive photoreactions take place in PAA (chain scission, crossslinking, and side groups abstraction). Although both polymers are also oxidised in case of exposure at air atmosphere but in PAA, the higher probability of chromophores formation in partially degraded and crosslinked chains is expected. The complete lack of photocrosslinking in PEO is the reason that formed chromophoric groups can be abstracted and evolved as low-molecular degradation product. As can be seen from UV–vis spectroscopic results, chromophore generation is much more efficient in PAA than that in PEO. Moreover, the formation of new chromophores in PAA and PAA-rich blends is more efficient than abstraction of carboxylic side groups. Hydrogen bonds do not protect the complexes against this reaction in PAA/PEO blends.

3.4. DSC and X-ray studies

The important topic in characterisation of photochemical processes in complexes, in which one of component is crystalline, is estimation of changes of crystallinity degree during UV-irradiation.

PEO shows a sharp melting peak at 70.1 °C in the DSC curve (Fig. 8). This peak is visible in the blend up to composition 50/50, but the minimum is shifted to lower temperature (about few degrees). In PAA, which is amorphous polymer, only glass temperature (126.7 °C) is observed in DSC thermograms. PAA-rich blends (>50% PAA) also do not exhibit melting endotherm, thus, the amount of free PEO chains capable to crystallization in these blends is not sufficient. It is obvious on the base of previous FT-IR study, which proved that numerous hydrogen bonds between PAA and PEO are formed.

One can conclude that degree of crystallisation melting temperature and microstructure of PEO are strongly perturbed by

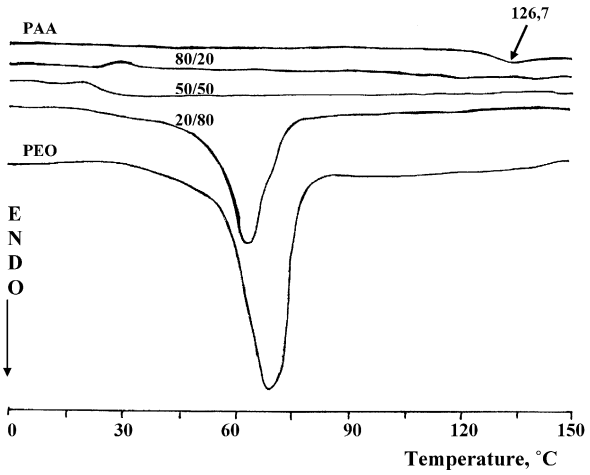

Fig. 8. DSC thermograms of pure components and PAA/PEO blends.

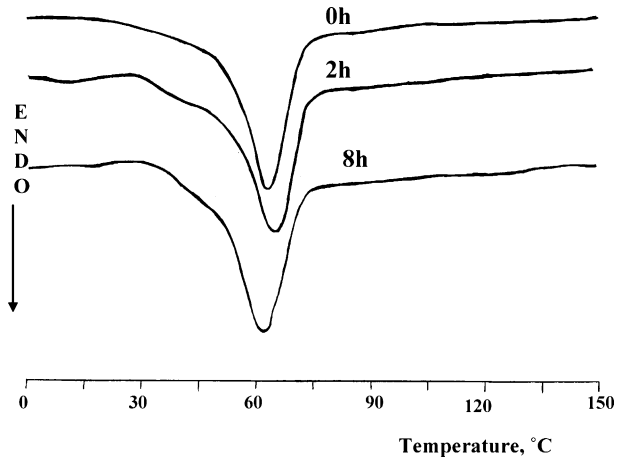

Fig. 9. DSC thermograms of PAA/PEO (20/80) blend before and after UV-irradiation (irradiation time: 0, 2 and 8 h).

the presence of amorphous PAA and specific interaction between components.

Table 2 shows the melting (T_m) and crystallization (T_c) temperature as well as crystallinity degree of PEO (X_c calculated according to formula 1) from DSC measurements for the blends with different composition.

Crystallisation (T_c) and melting (T_m) temperatures of unirradiated PEO were 42 and 70 °C, respectively. The PEO glass transition temperature (T_g) was not obtained by DSC in this condition because we had no possibility to cool the system below 0 °C; the reported T_g for PEO is −60 °C [26].

Pure PAA has $T_g \cong 127$ °C. The T_g of PAA shifts to lower values with the increase of the PEO amount in composition, suggesting miscibility. Only one glass transition temperature was observed for PAA/PEO blends (with composition: 90/10–50/50), within the detection limit of applied DSC. For other samples, in which expected T_g is below room temperature, T_g was not measured.

The theoretical (determined by the Fox equation) and experimental T_g values plotted versus complex composition coincide, confirming miscibility between the components in compositions studied. Although, this conclusion is done only on the base of few experimental points (because of temperature limitation in our DSC), we have additional data from literature supporting the miscibility of PAA and PEO in whole range of composition [13,27,28].

UV-irradiation causes the shift of PEO melting endotherms to lower temperatures (Fig. 9). Simultaneously, the peaks became broader. It is an evidence of changes of crystallities size and the degree of dispersion of ordered areas. It was previously suggested on the base of microscopic studies, that UV-irradiation causes the increase of spherulities size in PAA/PEO blends [29]. However, the changes of T_c and T_m caused by UV-irradiation in all PEO-rich samples are inconsiderable. Decrease of these temperatures after 8 h irradiation is probably results from a low-molecular photodegradation products formed.

The crystallinity degree (X_c) in pure PEO and blends with PEO high amount (80%) increases during UV-irradiation (Table 2), which is caused by higher chain mobility of shorter degraded chains and their tendency to regular packaging. However, in UV-irradiated PAA/PEO (50/50) complex, X_c value slightly decreases (Table 2). Similar behaviour was found for other UV-irradiated blend of PEO with PVC [23].

DSC results were confirmed by diffraction. An example of X-ray diffraction patterns of PEO and its blends containing 40–90% PEO are shown in Fig. 10. Crystalline peaks at $2\theta = 19°10'$ and $23°19'$, characteristic for PEO, appear also in the blends (up to 50% PEO). The lower amount of PEO in complex (<50%) do not allows to detect these X-ray patterns. Also the results of X-ray spectrometry for UV-irradiated PAA/PEO complexes are in good accordance with DSC data.

3.5. Thermogravimetric analysis

For estimation of thermal stability, all samples were subjected thermogravimetric analysis at nitrogen atmosphere. The

Table 2
Thermal parameters of PAA, PEO and their blends from DSC measurement (T_m, melting temperature; T_c, crystalization temperature; T_g, glass temperature; ΔH_{fus}, enthalpy of melting; ΔH_c, enthalpy of crystallization; X_c, crystallinity degree)

Sample composition PAA/PEO	T_m (°C) Before irradiation	ΔH_{fus} (J/g)	X_c (%)	T_c (°C)	ΔH_c (J/g)	T_g (°C)	ΔH_{fus} (J/g) After 8 h UV	X_c (%)
100/0	–	–	–	–	–	126.7		
80/20	–	–	–	–	–	32.1		
50/50	67.0	6.1	3.0	50.1	10.3	25.0	4.4	2.2
20/80	62.8	80.4	39.5	30.9	69.7	–	94.7	46.5
0/100	70.1	121.3	59.6	41.9	126.4	–	152.4	74.9

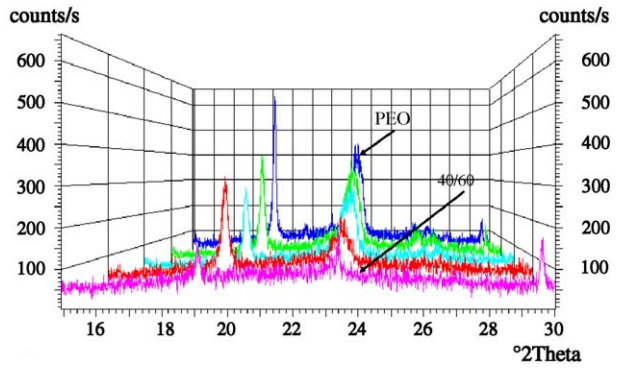

Fig. 10. X-ray diffraction of PEO and PAA/PEO blends (20/80, 40/60) (print version) and (10/90, 20/80, 30/70,40/60) (web version).

dependence of weight loss of PEO, PAA and their blends versus temperature is shown in Fig. 11. It is clearly seen that PEO thermal decomposition is one step process, whereas three stages of decay were observed in case of PAA and PAA/PEO complexes. The first small drop of weight about 100 °C is caused by removing of absorbed water residue (this process is omitted in our considerations). Next step beginning at 186 °C corresponds to breaking of chemical bonds in side groups with formation of cyclic structures (glutaric unhydride) and further water elimination. The third step staring at 314 °C is connected with destruction of carboxylic groups and CO_2 evolution as well as main chain scission. Moreover, other secondary degradation products containing ketonic, aldehydes and anhydride groups are formed at higher temperature [30]. During thermal decomposition of PEO, the breaking of C–C and C–O bonds in main chain occur [31].

The thermal degradation is almost complete in unexposed PEO (coal residue at 420 °C is about 3%), while in PAA this process is stopped after about 80% weight loss (at 500 °C). The blends are characterised by 80–95% weight loss and shifted decomposition temperature (T_{d1}) comparing to both pure polymers (Table 3). As can be seen PAA is less stable than PEO because of lower T_{d1} (T_{d1} for PAA is 186 °C but for PEO is 313 °C). Also complexes have lower T_{d1} (161–182 °C) than both pure polymers, which means that they are less thermally

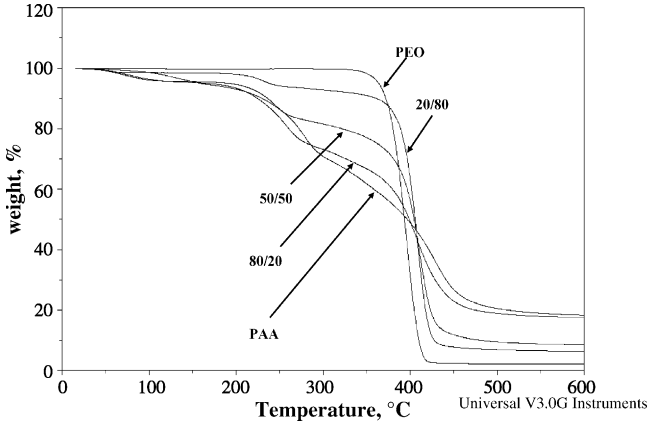

Fig. 11. Thermogravimetric curves for PAA, PEO and PAA/PEO complexes; obtained in nitrogen atmosphere.

Table 3
Decomposition temperature (T_{d1}) and weight loss (Δm_1) of PAA, PEO and their blends before and after UV-irradiation during 2 and 8 h from TGA measurement (for first main step of decomposition)

Sample composition PAA/PEO	T_{d1} (°C)			Δm_1 (%)		
	0 h	2 h	8 h	0 h	2 h	8 h
100/0	186	178	157	25.84	25.22	24.60
80/20	161	151	152	20.48	21.53	21.08
50/50	173	175	172	12.93	12.82	11.48
20/80	182	190	179	4.62	4.38	4.01
0/100	313	320	322	97.26	97.37	93.44

Table 4
Decomposition temperature (T_{d2}) and weight loss (Δm_2) of PAA, PEO and their blends before and after UV-irradiation during 2 and 8 h from TGA measurement (for second main step of decomposition)

Sample composition PAA/PEO	T_{d2} (°C)			Δm_2 (%)		
	0 h	2 h	8 h	0 h	2 h	8 h
100/0	314	312	300	49.12	50.59	51.63
80/20	299	294	297	52.19	55.97	58.18
50/50	301	284	285	76.98	73.65	74.30
20/80	268	264	272	87.29	86.21	88.16

stable. The T_{d1} in blends increases with the increase of PEO content.

UV-irradiation leads to T_{d1} drop in PAA and PAA-rich blends, whereas in PEO this temperature increases about few degrees. In other PAA/PEO blends, T_{d1} changes are irregular. The changes of the weight loss (Δm_1) during UV-irradiation are inconsiderable. The decrease of Δm_1 in pure PAA and PEO after UV-irradiation indicates that before thermal degradation some low-molecular photoproducts were evolved. The Δm_1 changes in UV-irradiated blends are smaller than that in pure PAA and PEO.

The complex with unimolar composition (50/50) seems to be most photoresistant among all complexes because of negligible changes in T_{d1} and Δm_1 parameters.

Analysing the second step of decay for blends with PAA dominant content, also the drop of T_{d2} was observed comparing to T_{d2} for pure PAA (Table 4). In most cases, UV-irradiation leads to further T_{d2} decrease. Somewhat higher Δm_2 values in 8 h UV-irradiated PAA and its complexes can lead to conclusion that chemical bonds became weaker upon UV action. The exception is PAA/PEO (50/50) blend, in which Δm_2 insignificantly decreases during exposure.

4. Conclusions

Mixing of PAA and PEO leads to formation of interpolymer complexes with hydrogen bonds between proton-donating PAA and proton-accepting PEO. The formation of hydrogen bonds induces polymer miscibility on molecular level, which was proved by FT-IR and DSC investigation. It is in accordance with literature data.

Although the strength and amount of hydrogen bonds between PAA and PEO is lower than self-associated hydrogen

bonds in PAA because of lower accessibility of oxygen atoms in PEO comparing to PAA, these bonds have a great influence on photochemical transformation in PAA/PEO complexes. Photooxidative degradation is hampered in PAA/PEO comparing to this reaction in pure components. Irregular changes observed in main absorption bands suggest competition between photochemical reactions occurring simultaneously in studied systems.

Crystallization of PEO is suppressed in the presence of higher amount of PAA (>50%) but the effect of UV-irradiation on crystallinity degree in these blends is negligible, contrary to PEO and in blends with its majority, where the increase of crystallinity was observed after exposure to UV.

PAA/PEO complexes are characterised by lower thermal stability than pure polymers. It means that hydrogen bonds, which play an important role in strengthening of complex structure, are broken during heating. The influence of UV-irradiation on thermal stability of PAA/PEO complexes is small. Thermogravimetric analysis indicates that unimolar PAA/PEO (50/50) complex is most photostable among other blends.

References

[1] H. Wang, W. Li, Y. Lu, Z. Wang, W. Zhong, J. Appl. Polym. Sci. 61 (1996) 2221.
[2] E. Tsuchida, K. Abe, Adv. Polym. Sci. 45 (1982).
[3] L. Xinya, R.A. Weiss, Macromolecules 28 (1995) 3022.
[4] J. Dong, Y. Ozaki, Macromolecules 30 (1997) 286.
[5] S.H. Jeon, T. Ree, J. Polym. Sci., Part A: Polym. Chem. 26 (1988) 1419.
[6] S. Kawaguchi, T. Kitano, K. Ito, Macromolecules 24 (1991) 6030.
[7] H. Kaczmarek, A. Szalla, A. Kamińska, Polymer 42 (2001) 6057.
[8] M.M. Coleman, J.F. Graf, P.C. Painter, Specific Interaction and the Miscibility of Polymer Blends, Technomic, London, 1991.
[9] M.M. Coleman, P.C. Painter, Prog. Polym. Sci. 20 (1995) 1.
[10] S. Połowiński, Wybrane Zagadnienia z Chemii Fizycznej Polimerów (The Chosen Problems of Polymer Physical Chemistry), Wydawnictwo Politechniki Łódzkiej, Łódź, 1997.
[11] P.C. Shannon, R.Y. Lochhead, Polym. Prep. ACS Div. Polym. Chem. 37 (1996) 471.
[12] M. Jiang, M. Li, Adv. Polym. Sci. 146 (1999) 121.
[13] Y. He, B. Zhu, Y. Inoue, Prog. Polym. Sci. 29 (2004) 1021.
[14] Ch. Lau, Y. Mi, Polymer 43 (2002) 823.
[15] E. Fekete, E. Földes, B. Pukánszky, Eur. Polym. J. 41 (2005) 727.
[16] R.K. Wanchoo, P.K. Sharma, Eur. Polym. J. 39 (2003) 1481.
[17] S.M. da Silva Neiro, D.C. Dragunski, A.F. Rubira, E.C. Muniz, Eur. Polym. J. 36 (2000) 583.
[18] L.A. Kanis, F.C. Viel, J.S. Crespo, J.R. Bertolino, A.T.N. Pires, V. Soldi, Polymer 41 (2000) 3303.
[19] A.M. Rocco, R.P. Pereira, M.I. Felisberti, Polymer 42 (2001) 5199.
[20] F. Li, M.V. Hanson, R.C. Larock, Polymer 42 (2001) 1567.
[21] S. Pimbert, L. Avignon-Poquillon, G. Levesque, Polymer 43 (2002) 3295.
[22] H. Kaczmarek, Polymer 37 (1996) 547.
[23] H. Kaczmarek, J. Kowalonek, Z. Klusek, S. Pierzgalski, S. Datta, J. Polym. Sci., Part B: Polym. Phys. 42 (2004) 585.
[24] G. Guerrica-Echevarría, J.I. Eguiazábal, J. Nazábal, Polym. Test. 19 (2000) 849.
[25] X.D. Huang, S.H. Goh, Polymer 43 (2002) 1447.
[26] J. Brandrup, E.H. Immergut, Polymer Handbook, 3rd ed., Wiley, New York, 1989.
[27] T. Miyoshi, K. Takegoshi, K. Hikichi, Polymer 38 (1997) 2315.
[28] X. Lu, R.A. Weiss, Macromolecules 18 (1995) 3022.
[29] H. Kaczmarek, A. Szalla, H. Chaberska, J. Kowalonek, Surf. Sci. 566 (2004) 560.
[30] I.C. Mc Neill, S.M.T. Sadeghi, Polym. Deg. Stab. 29 (1990) 233.
[31] G.G. Cameron, M.D. Ingram, M.Y. Qureshi, H.M. Gearing, Eur. Polm. J. 25 (1989) 779.